Linear stability analysis of three-dimensional lid-driven cavity flow

Flavio Giannetti[1], Paolo Luchini[1], Luca Marino[2]
[1]*Department of Mechanical Engineering, University of Salerno, Italy*
E-mail: luchini@unisa.it, fgiannetti@unisa.it

[2]*Department of Mechanics and Aeronautics, University of Rome "La Sapienza", Italy*
E-mail: luca.marino@uniroma1.it

Keywords: Vortex flows, Linear stability.

SUMMARY. In this paper we present the results of a linear stability analysis applied to an incompressible flow in a three dimensional lid-driven cavity. The principal goal is the evaluation of the critical value of the Reynolds number and the main characteristics of the flow instability.

1 INTRODUCTION

The analysis of an incompressible flow in a squared lid-driven cavity is classical in fluid mechanics. In spite of the fact that is one of the most studied problem in this discipline, it is still an interesting and challenging task if the three dimensional case is considered.

Starting from about 1960 [1, 3, 4], the interest of the researchers focused on the main characteristics of the two-dimensional cavity. In particular, the effect of the Reynolds number on the size of the principal vortex and the rise and development of the secondary eddies were considered in a great number of published papers. The review article [5] reports the state of the art about the physics of the cavity flow up to the end of the century. Moreover the complexity of the phenomenon pushed many authors to adopt this problem as a test for numerical algorithm and to produce benchmark solution. Among the others, those published by Ghia et al. and then by Schreiber at al. [6, 7], in the two dimensional geometry, are still referenced.

Questions about the stationarity and/or uniqueness of the flow, as well as the development of instabilities have been approached quite recently.

Following a linear approach to the stability problem, the three-dimensional instability of a two dimensional base flow has been studied by several authors [8, 9, 10] by means of the normal modes hypothesis. The critical values of the Reynolds number was evaluated correctly by Albensoeder et al. [10] as about 786, with a corresponding spanwise wave number equal to 15.8.

When both the base flow and the perturbation field are two-dimensional, the critical Reynolds number is higher and has been calculated by Auteri et al. [11] in the range [8017.6,8018.8].

The interest on the three-dimensional flow arose around 1970 (i.e. [12]) and several papers described the topology of the flow in cavities with different aspect ratio (see [13, 14, 15] for example).

By marching in time the nonlinear 3D Navier-Stokes equations in a cubic cavity, Iwatsu et al. [16] observed unsteady flows for Reynolds numbers above 2000, but their results were not conclusive about the onset of an instability. According to their numerical results they observed a change in the behavior of the flow in the quite wide range 2000-3000.

The stability of the three-dimensional base flow was recently studied numerically by Kuhlmann et al. [17] who considered both periodic and no-slip boundary conditions in the spanwise direction. In particular, the case of no-slip boundaries was investigated only for an aspect ratio equal to 6.55 and the results were compared against experimental data and the 3D stability analysis performed on a 2D base flow.

At the best of the authors knowledge the stability of the case of a cubic cavity with rigid walls has not been solved yet. For this reason the main goal of this paper is to evaluate, in the framework of the linear stability theory, the critical value of the Reynolds number and to investigate the behavior of the most important modes as a function of the Reynolds number.

In the next section the problem and the corresponding equations are formulated. Then the numerical approach that has been adopted is described pointing out the main differences with the previous numerical technique. In the last section the main properties of the base flow and the perturbation field are shown and discussed.

2 PROBLEM FORMULATION

We consider an incompressible Newtonian fluid, with constant dynamic viscosity μ, in a cubic cavity of sizes $L \times L \times L$, in the x, y, z-space. The flow is driven by the motion of the wall located at $y = L$ with constant velocity $\mathbf{V} = V\mathbf{e_x}$.

In such hypotheses, the Navier-Stokes equations, governing the flow motion, are

$$\frac{\partial \mathbf{v}}{\partial t} + \nabla \cdot (\mathbf{v}\mathbf{v}) = -\nabla p + \frac{1}{Re}\nabla^2 \mathbf{v}, \qquad (1)$$
$$\nabla \cdot \mathbf{v} = 0.$$

The definition of the Reynolds number $Re = \rho V L/\mu$, where ρ is the constant density of the fluid, completes the formulation of the problem.

The linear stability analysis is obtained by the decomposition of the flow field in a base, stationary and three-dimensional flow $(\bar{\mathbf{v}}, \bar{p})$ and a small amplitude, time dependent, three-dimensional perturbation $(\mathbf{v}', p')$.

The base flow $(\bar{\mathbf{v}}, \bar{p})$ satisfies the steady version of equations (1), with the following boundary conditions:

$$\bar{\mathbf{v}}(x = 0) = 0 \quad , \bar{\mathbf{v}}(x = L) = 0$$
$$\bar{\mathbf{v}}(y = 0) = 0 \quad , \bar{\mathbf{v}}(y = L) = V\mathbf{e_x}$$
$$\bar{\mathbf{v}}(z = 0) = 0 \quad , \bar{\mathbf{v}}(z = L) = 0$$

The perturbation field $(\mathbf{v}', p')$ is governed by the following set of linearized Navier-Stokes equation,

$$\frac{\partial \mathbf{v}'}{\partial t} + \bar{\mathbf{v}} \cdot \nabla \mathbf{v}' + \mathbf{v}' \cdot \nabla \bar{\mathbf{v}} + \nabla p' = \frac{1}{Re}\nabla^2 \mathbf{v}' \qquad (2)$$
$$\nabla \cdot \mathbf{v}' = 0$$

with homogeneous boundary conditions.

Solutions of the Eq.(2) are searched as normal modes

$$[\mathbf{v}'(x, y, z, t), p'(x, y, z, t)] = [\hat{\mathbf{v}}(x, y, z), \hat{p}(x, y, z)] \exp[\sigma t] + c.c. \qquad (3)$$

where $\sigma \in \mathbb{C}$ is the eigenvalue and $c.c.$ means the complex conjugate of the preceding expression. The real part of σ gives the growth or decay rate of the mode, while the imaginary part describes the oscillating nature of the mode.

Both the base flow and the stability equations, both written in a conservative form, are discretized by mean of a second order centered finite-difference scheme on a smoothly varying staggered grid. In order to capture the boundary layers forming at high Reynolds number, points are clustered near

the walls by using a quadratic mapping: in this way the grid spacing in the center of the cavity is approximately 8-10 times larger than in the wall regions.

The base flow calculations are performed with a multigrid solver employing FAS and the classical DGS Vanka smoother. In order to achieve fast convergence a first order upwind discretization for the convective terms is needed in the smoother, while a deferred correction outer iteration is used to drive the residual of the second order discretization to machine precision. For smaller grids, the results were validated with the solutions obtained by a direct approach in which a classical Newton-Raphson procedure and a sparse LU-solver (UMFPACK) was used to solve the nonlinear algebraic equations derived by the discretization.

Once the base-flow was calculated, the stability analysis was performed by marching the linearized equations in time and using the ARPACK library in order to determine the leading Floquet multipliers of the system. In particular, a Crank-Nicholson scheme was adopted for the time discretization, leading at each time step to a linear set of equations which was solved with a multigrid scheme similar to that used for the base-flow calculations. Since the convective terms were treated implicitly, no stability restriction on the temporal time steps had to be imposed. This is an important point, especially when a stretched grid is adopted. In order to validate the results, a different approach was also used. In particular, a new algorithm based on a subspace iteration coupled with a multigrid solver and a SIMPLE smoother was adopted to extract the leading modes of the system. Details of the algorithm can be found in ([2]). For the driven cavity case this last procedure was slightly faster than the approach based on a time-marching scheme and the ARPACK library. Finally on the smaller grids, the results obtained by the two iterative schemes were also validated by using a classical inverse-iteration algorithm, were at each iteration a large sparse matrix was inverted with the UMFPACK LU solver.

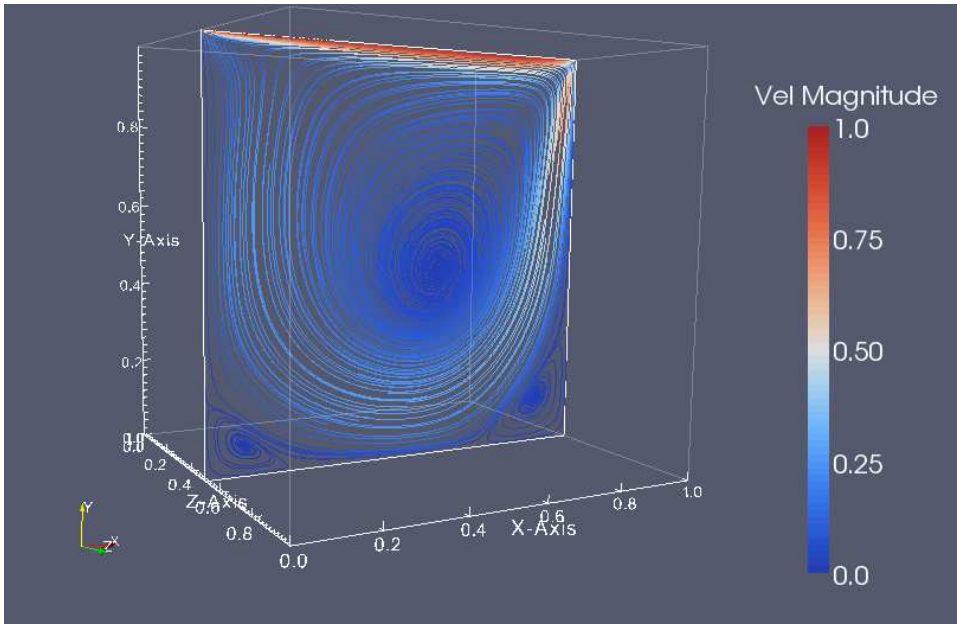

Figure 1: Streamlines of the base flow in the symmetry plane $z = 0.5$ and $Re = 1000$.

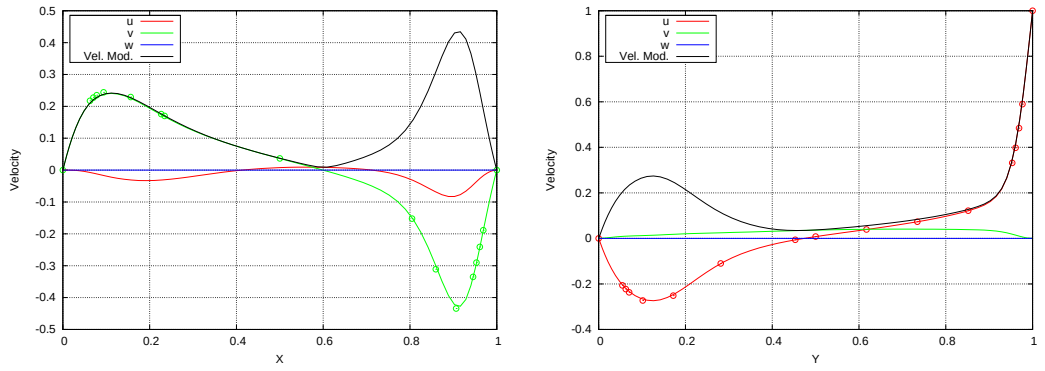

(a) (b)

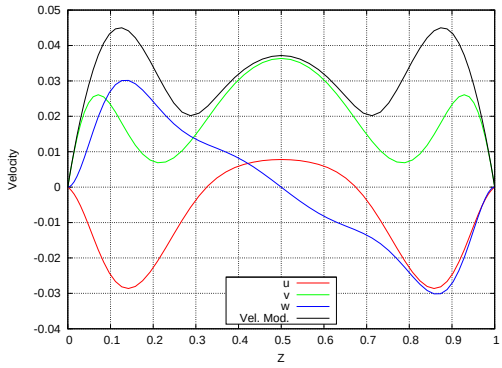

(c)

Figure 2: Velocity profiles of the base flow on the centerlines of the cavity. (a): $(x, 0.5, 0.5)$, (b):$(0.5, y, 0.5)$, (c):$(0.5, 0.5, z)$. $Re = 1000$

3 RESULTS

3.1 Base Flow

Calculations were performed for several Reynolds numbers using two different grids: a smaller one containing $32 \times 32 \times 32$ points and a larger one with $64 \times 64 \times 64$ points. The results obtained at different resolutions do not show any appreciable difference. For all the Reynolds numbers investigated the base-flow shows a complex 3D structure with a symmetry plane located at $z = 0.5$, where the spanwise velocity component w is zero.

As an example, Figure 1 shows the streamlines in the plane of symmetry for $Re = 1000$. The solution consists of a primary main 3D vortex located in the center of the cavity, together with two smaller eddies arising in the corners of the stationary walls. As the Reynolds number is further increased a third eddy emerges close to the upper part of the left vertical wall.

A comparison with the two-dimensional case (see for example [6]) shows that close to the symmetry plane the 3D flow has qualitatively the same behavior as the 2D solution. Quantitative differences however exist and are due to the spanwise distribution of the w velocity component. Large qualitative deviations from the 2D solution, instead, are observed close to the two vertical walls parallel to the symmetry plane. In these regions, in fact, the no-slip conditions force the velocity components to vanish.

Figures 2 and 3 report the profiles of the three velocity components, as well as its modulus, on

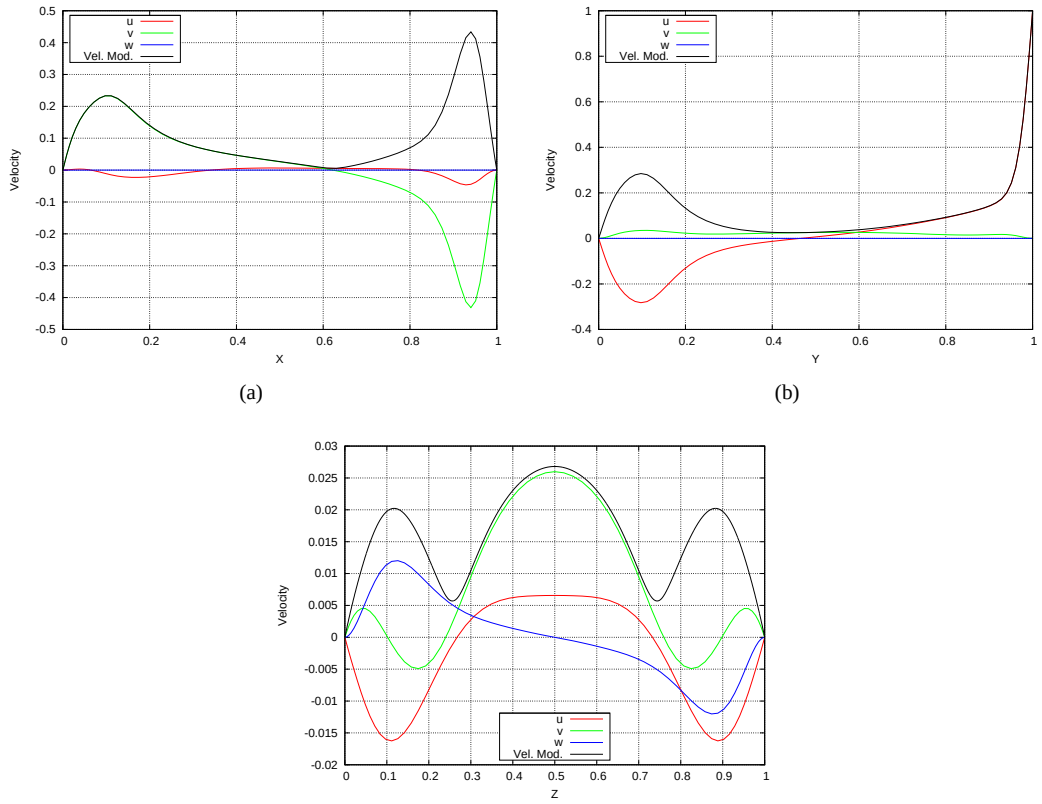

Figure 3: Velocity profiles of the base flow on the centerlines of the cavity. (a): $(x, 0.5, 0.5)$, (b):$(0.5, y, 0.5)$, (c):$(0.5, 0.5, z)$. $Re = 2000$

the centerlines of the cavity, in the two cases $Re = 1000$ and $Re = 2000$. Due to the symmetry at $z = 0.5$ ((a) and (b) of Figs.2,3) the w component is identically zero in these pictures, while on the centerline $(0.5, 0.5, z)$ normal to the symmetry plane the distributions is symmetrical for u and v, and anti-symmetrical for w.

On Fig. 2 we also reported, as small circles, the results of [18] where accurate numerical calculations have been carried out for the base flow at $Re = 1000$. The agreement between the two set of data is very satisfactory.

3.2 Stability

The stability analysis was performed for different values of the Reynolds numbers by using the iterative algorithms described in the introduction. In particular, the first 10 dominant modes were computed for values of Re equals to 10, 100, 500 800 1000, 1250, 1500, 1750, 2000 and 2100. According to the stability analysis, the steady symmetric base-flow described in the previous section becomes unstable for $Re > 2000$. This result was also confirmed by marching in time the nonlinear 3D Navier-Stokes equations and checking for which Re the flow reached a steady state.

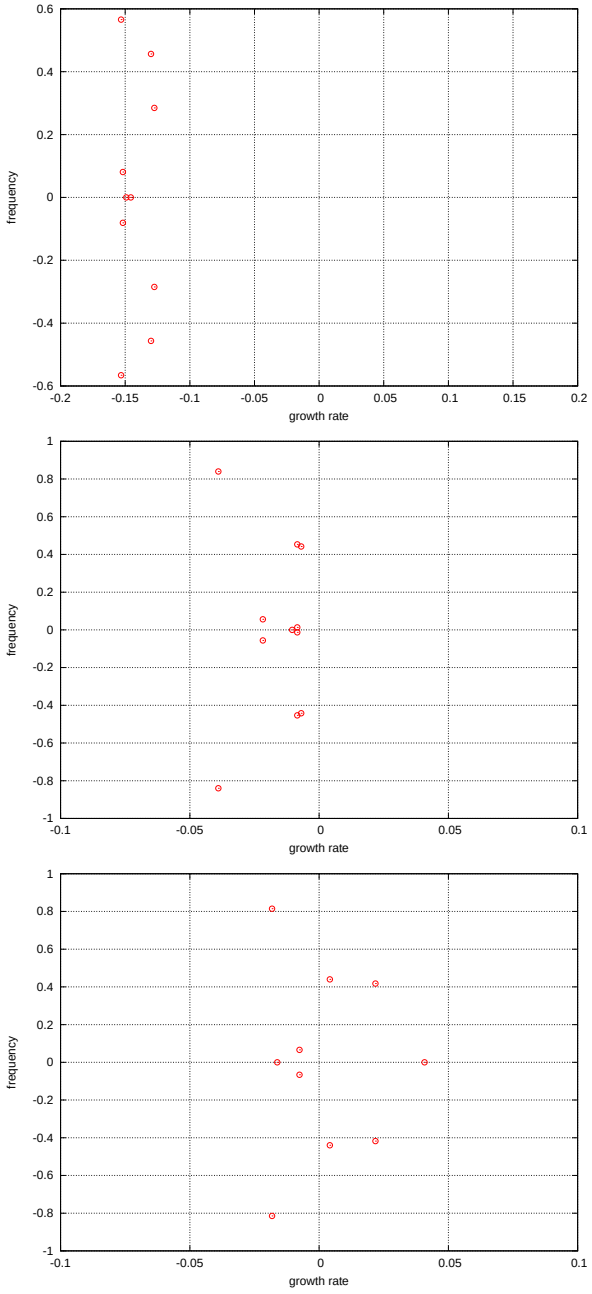

Figure 4: Eigenvalues distribution in the complex plane. Top: $Re = 1000$. Middle: $Re = 2000$. Bottom: $Re = 2100$.

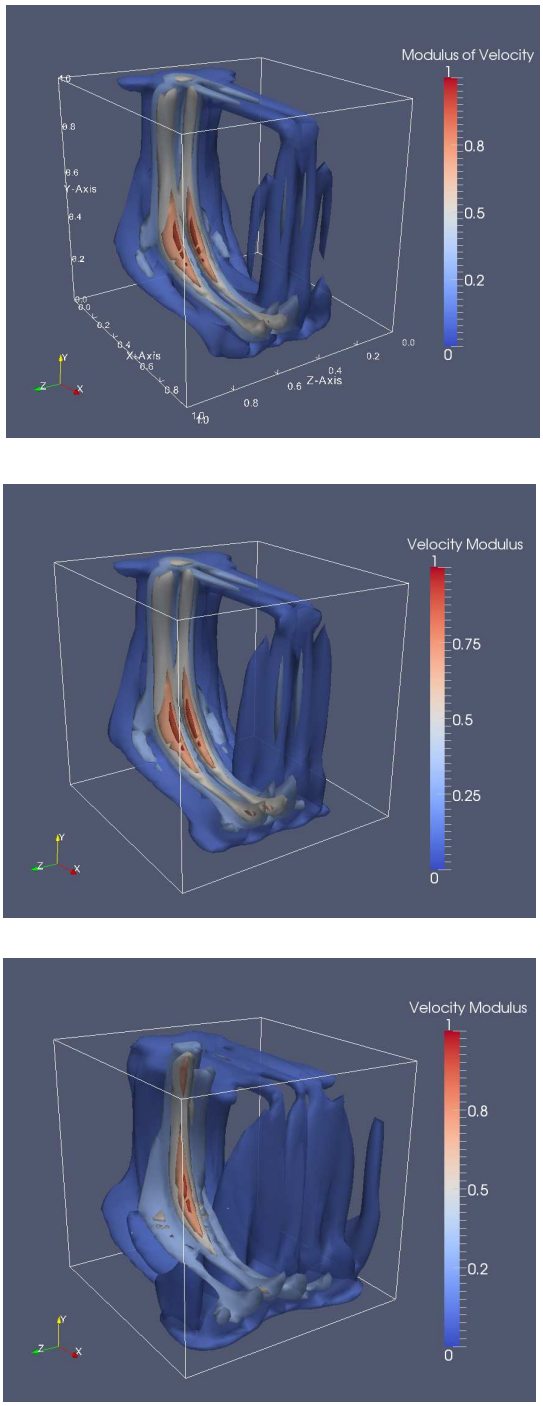

Figure 5: Contour surfaces of $|\mathbf{v}'|$ of the first unstable modes. $Re = 2100$. Top: $\sigma_r = 0.040$, $\sigma_i = 0$. Middle: $\sigma_r = 0.022$, $\sigma_i = 0.417$. Bottom: $\sigma_r = 0.0042$, $\sigma_i = 0.44$.

Simulations were started using as initial condition a small random fluctuation superposed to the steady solution previously computed. The stability characteristics of the flow can be easily inferred by looking at the spectra for different Reynolds numbers. As an example, Fig. 4 shows the results

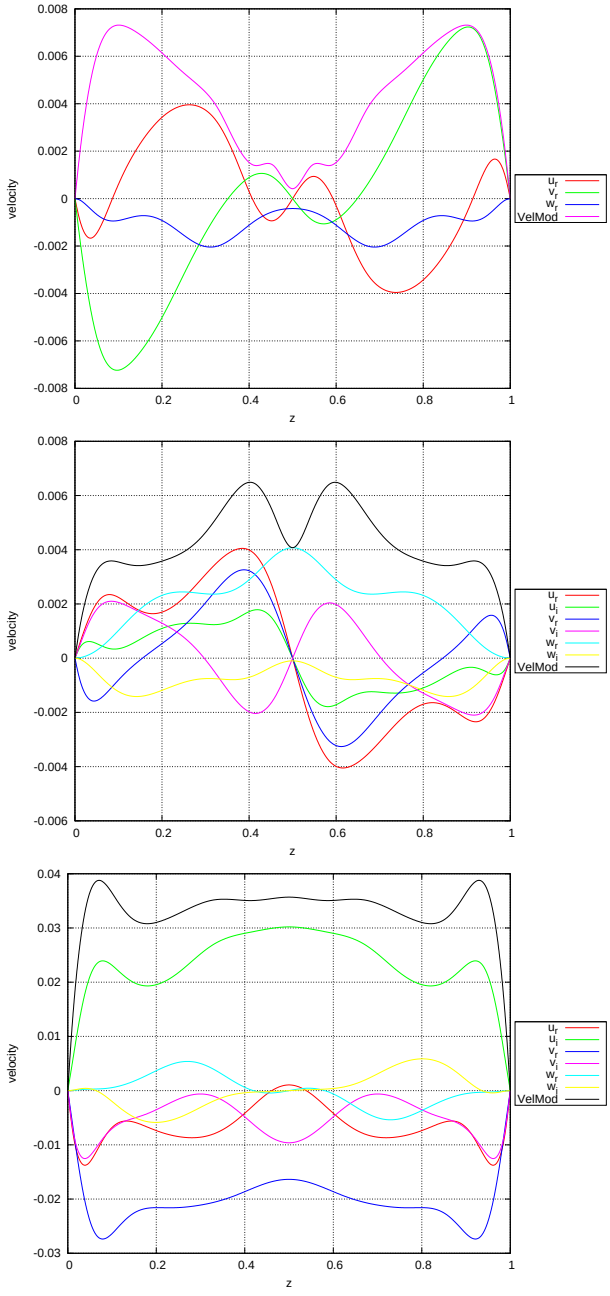

Figure 6: Profiles of the real and imaginary part of the velocity of the first unstable modes on the centerlines. $Re = 2100$. Top: $\sigma_r = 0.040$, $\sigma_i = 0$. Middle:$\sigma_r = 0.022$, $\sigma_i = 0.417$. Bottom: $\sigma_r = 0.0042$, $\sigma_i = 0.44$.

for $Re = 1000, 2000, 2100$. As noticed also in [16], where the flow in a 3D cubic lid-driven cavity was investigated, in the neighborhood of $Re = 2000$ the flow changes its behavior. According to our stability analysis the least damped mode (a stationary mode), in fact becomes unstable just above $Re \approx 2000$.

Note that for all the Reynolds numbers considered in our analysis, both stationary and oscillating modes were found and, at $Re = 2100$, the most unstable one is stationary. In order to better understand the spatial structure of these modes, the iso-surface contours of the modulus of the velocity are shown in Fig.4. In particular the first picture (Top of Fig.5) refers to the unstable stationary mode, while the other two graphics refer to to the oscillating unstable modes. In all cases, the perturbation field is localized around the plane $z = 0.5$ (plane of symmetry for the base flow) in proximity of the secondary eddy near the corner. The the fluctuating perturbations related to third unstable mode are less localized and show a more complex spatial structure.

While the distributions reported in Fig.5, concerning the modulus of the velocity, show a symmetrical behavior, the profiles of the individual components of both the real and imaginary parts of the velocity reveal the symmetric or anti-symmetric nature of the instabilities. Fig.6 (Top) refers to the stationary mode and shows that the w component is symmetrical with respect to the plane $z = 0.5$ and the u and v components are anti-symmetric. This behavior is opposite to what we observed for the base-flow. Thus, the appearance of such instability is also associated with a loss of symmetry of the steady solution. Similar spatial characteristics are observed for the second mode (Fig. 6 Middle) where both the real and the imaginary parts are reported while an opposite behavior can be noticed for the third mode (Fig.6 Bottom).

References

[1] Moffatt, H.K., "Viscous and resistive eddies near a sharp corner," *J. Fluid Mech.*, **18**, 1-18 (1964).

[2] Luchini, P., Giannetti, F., Pralits, J., "An iterative algorithm for the numerical computation of bluff-body wake instability modes and its application to a freely vibrating cylinder," *Fifth Conference on Bluff Body Wakes and Vortex-Induced Vibrations 12-15 December 2007 Costa do Saupe, Bahia, Brazil* , **18**, 1-18 (2007).

[3] Burggraf, O.R., " Analytical and numerical studies of the structure of steady separated flows," *J. Fluid Mech.*, **24**, 113-151 (1966).

[4] Pan, F., Acrivos, A., "Steady flows in rectangular cavities," *J. Fluid Mech.* **28**, 643-655 (1967).

[5] Shankar, P.N., Deshpande, M.D., " Fluid mechanics in the driven cavity," *Annu. Rev. Fluid Mech.*, **32** 93-136 (2000).

[6] Ghia U., Ghia, K.N., Shin, C.T., "High-Re solutions for incompressible flow using the Navier-Stokes equations and a multigrid method," *J. Comput. Phys.*, **48** 387-411 (1982).

[7] Schreiber, R., Keller, H.B., "Driven cavity flows by efficient numerical techniques," *J. Comput. Phys.*, **49** 310-333 (1983).

[8] Ramanan, N, Homsy, G.M., "Linear stability of lid-driven cavity flow," *Phys. of Fluids*, **6** 2690-2701 (1994).

[9] Ding, Y., Kawahara, M., “Three-dimensional linear stability analysis of incompressible viscous flows using the finite element method,” *Int. J. Numer. Meth. Fluids*, **31** 451-479 (1999).

[10] Albensoeder,S. Kuhlmann, H.C., Rath, H.J., ”Three-dimensional centrifugal-flow instabilities in the lid-driven cavity problem,” *Phys. Fluids*, **13** 121-135 (2001).

[11] F. Auteri, N. Parolini, L. Quartapelle, “ Numerical investigation on the stability of singular driven cavity flow,” *J. Comput. Phys.*, **183**, 1-25 (2002).

[12] G. De Vahl Davis, G.D. Mallinson, “An evaluation of upwind and central difference approximations by a study of recirculating flow,” *Comp. Fluids*, **4**, 29-43 (1976).

[13] T.P. Chiang, W.H. Sheu, R.R. Hwang, “Three-dimensional vortex dynamics in a shear-driven rectangular cavity,” *Int. J. Comput. Fluid Dyn.*, **8** 201-214 (1997).

[14] T.P. Chiang, W.H. Sheu, R.R. Hwang, “Effect of Reynolds number on the eddy structure in a lid-driven cavity,” *Int. J. Num. Meth. Fluids*, **26**, 557-579 (1998).

[15] T.W.H. Sheu, S.F. Tsai, “Flow topology in a steady three-dimensional lid-driven cavity,” *Comput. Fluids*, **31**, 911-934 (2002).

[16] R.Iwatsu, K. Ishii, T. Kawanura, K. Kuwahara, “Numerical simulation of three-dimensional flow structure in a driven cavity,” *Fluid Dyn Res.*, **5**, 173-189 (1989).

[17] Albensoeder,S. Kuhlmann, H.C., ”Nonlinear three-dimensional flow in the lid-driven square cavity,” *J. Fluid Mech.*, **569** 465-480 (2006).

[18] Albensoeder,S. Kuhlmann, H.C., ”Accurate three-dimensional lid-driven cavity flow,” *J. Comp. Phys.*, **206** 536-558 (2005).